Journal of Nuclear Materials 377 (2008) 348–351

Contents lists available at ScienceDirect

Journal of Nuclear Materials

journal homepage: www.elsevier.com/locate/jnucmat

Effects of transmutation elements on the defect structure development of W irradiated by protons and neutrons

J.C. He [a,*], A. Hasegawa [b], K. Abe [b]

[a] NAMI, The Hong Kong University of Science and Technology, Clear Water Bay, Kowloon, Hong Kong, PR China
[b] Department of Quantum Science and Energy Engineering, Tohoku University, Sendai, Japan

ARTICLE INFO

Article history:
Received 30 October 2007

ABSTRACT

A series of W–Re–Os alloys were fabricated by arc melting for investigating the effects of transmutation elements of tungsten on the defect structure development. Transmutation electron microscopy has been used to investigate the defect structure for proton-irradiated (E = 1 MeV) W, W–3Re, W–3Os and 0.15 dpa neutron-irradiated (E > 1 MeV) W–5Re–3Os and W, W–3Re, W–5Re and W–26Re. The irradiation-induced voids and dislocation loops which directly cause the irradiation hardening were observed. The results show the combination of W with Re or Os effectively restrains irradiation damage since the number density and radius of both voids and dislocation loops remarkably decrease with increasing Re or Os content.

1. Introduction

The need for materials capable of operating at high temperatures in fusion reactors has focused attention on the body-centered cubic refractory metals and alloys. Tungsten (W) has been considered as one of the candidate materials for plasma-facing components (PFCs) of the fusion reactor [1–3]. Under 14 MeV-neutron irradiation conditions in fusion reactors, large amounts of solid transmutation products, mainly including rhenium (Re) and osmium (Os), will be produced from the transmutation actions of W [4,5], and this reaction will cause the sigma phase formation. Cottrell [6] had determined a reaction pathway for W to Re and Os under 14 MeV-neutron irradiation with a wall loading of 2 MW m^{-2}. The result showed that the pure W was expected to be (atomic percentage): W 75.1; Os 12.8; Re 11.9, plus small amounts of other elements. As part of the effort to evaluate the effects of these transmutation products on W in nuclear environments, a series of W–Re–Os alloys has been fabricated and transmission electron microscopy has recently been utilized for direct observation of radiation-induced microstructure features.

On the other hand, previous work showed W–26 wt% Re neutron-irradiated to 11 dpa featured significant hardening and embrittlement because radiation-induced precipitation of σ (ReW) (30–55 at.% W) and χ (Re_3W) phases were massively generated [7,8]. The present work aims to clarify the roles of transmutation products of Re or Os in lower dose irradiation environments. As an effect evaluation, we carried out both the proton and neutron irradiation for the W-based alloys, respectively. A discussion on comparison of neutron-irradiated with proton-irradiated effects on W-based alloys under the same irradiation dose was also included.

2. Experimental

The proton-irradiated W, W–3Re, W–3Os and W–5Re–3Os (wt%) alloys were fabricated by gas tungsten arc (GTA) melting [9]. The neutron-irradiated W, W–3Re, W–5Re and W–26Re (wt%) alloys were supplied by the Plansee Cooperation. Table 1 shows the chemical composition of all alloys used for the present work. TEM disks (3 mm in diameter × 0.2 mm in thickness) were prepared and annealed at 1400 °C for 3600 s in an evacuated quartz tube (<10^{-5} Pa) before both irradiations. The 1 MeV proton irradiation was carried out by the Dynamitron Accelerator at Tohoku University. The damage rate was about 2.1×10^{-5} dpa/s, and the irradiation temperature measured by an infrared pyrometer was at 500 and 600 °C within an error region of ±10 °C. These irradiation experiments were conducted in vacuum of less than 3.7×10^{-4} Pa. Fig. 1 shows the depth distribution of displacement damage calculated by the TRIM code [10]. The damage structure was uniformly created from the surface to a depth of about 3 μm. Microstructural observations selected a target layer at depth of 2 μm obtained with the displacement damage of 0.15 dpa. The neutron irradiation was carried out in irradiation cycles of 98M-7U in the JMTR (Japan Materials Test Reactor) at 600 °C to 0.15 dpa. The neutron fluence was up to 3.7×10^{24} n/m^2 (E_n > 1 MeV). Neutron and proton-irradiated disks were prepared using a twin-jet and a single-jet polishing machine, respectively, with a solution of 1 wt% NaOH at room temperature. A Hitachi HF-2000 Transmission Electron Microscopy and a JEOL JEM-2010 Transmission Electron Microscopy operated at 200 kV were

* Corresponding author. Tel.: +852 23588119; fax: +852 35210618.
E-mail address: hejianch@ust.hk (J.C. He).

0022-3115/$ - see front matter
doi:10.1016/j.jnucmat.2008.03.014

Table 1
Chemical compositions of irradiated W and W-based alloys (wt%)

Materials	W	Re	Os	O	N	C
Proton-irradiated (fabricated by arc melting)						
W	Bal.	–	–	0.0039	<0.0006	0.0017
W–3Re	Bal.	3.3	–	0.0023	<0.0006	0.0009
W–3Os	Bal.	–	3.2	0.0021	<0.0006	0.0190
W–5Re–3Os	Bal.	4.9	3.3	0.0032	<0.0006	0.0046
Neutron-irradiated (supplied by Plansee Corp.)						
W	Bal.	–	–	0.0024	<0.001	0.0011
W–3Re	Bal.	3	–	0.0017	<0.001	0.0006
W–5Re	Bal.	5	–	0.0036	<0.001	0.0016
W–26Re	Bal.	26	–	0.0015	<0.001	0.0008

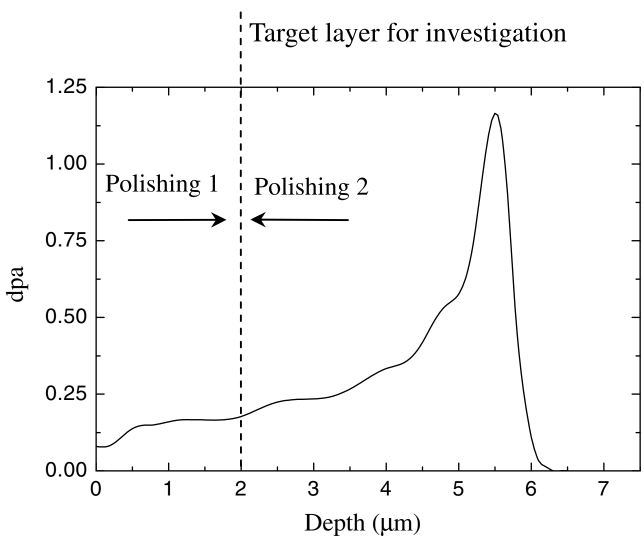

Fig. 1. Depth distribution of displacement damage for proton in tungsten calculated by the TRIM code. A single-jet polishing machine and laser microscopy with thickness measurement system were used for preparation of the proton-irradiated disks.

employed for investigating proton and neutron-irradiated samples, respectively. Number density and radius of radiation-induced voids and loops were examined on TEM photographs by the Table-J86 program that was performed on N88-DiskBasic system. The Vickers microhardness was measured at room temperature under a load of 1.96 N over 30 s.

3. Results

3.1. Proton irradiation

Fig. 2 compares the microstructures under bright-field kinematic condition while the diffraction vector is $g = [200]$. Defect clusters featured as loops and rafts were observed in W and W–3Re proton-irradiated to 0.15 dpa at 500 and 600 °C, respectively. No loops were observed in the proton-irradiated W–3Os and W–5Re–3Os. Fig. 3 shows the proton irradiation-induced voids in W, W–3Os and W–5Re–3Os at 500 °C and in W–3Re at 600 °C. The voids in each irradiated sample were observed, but their size and number density are obviously different. Both solute Re and solute Os play the role of reducing the void size with a corresponding decrease in density. The voids in irradiated W–3Os are very small, and the largest and more spherical voids are given in irradiated W–3Re at 600 °C. Fig. 3(d) shows voids in irradiated W–5Re–3Os which are little bigger than those in W–3Os even with 5% Re addition.

3.2. Neutron irradiation

Fig. 4 shows dislocation loops in W, W–3Re, W–5Re and W–26Re neutron-irradiated at 600 °C to 0.15 dpa while the diffraction vector is $g = [200]$. There is a significant restraining effect on nucleation and growth of loops given by the Re. The neutron irradiation-induced voids in W, W–3Re, W–5Re and W–26Re are illustrated in Fig. 5. The restraining effect on the growth of voids is also featured, but it is not progressively improved with increasing Re content. Both the voids and loops were not observed in irradiated W–26Re.

The examinated results of size and number density of radiation-induced loops and voids by neutron and proton irradiation to 0.15 dpa is summarized in Table 2. As contrasted with the neutron irradiation, the proton irradiation trends to induce higher density and bigger size of voids with a corresponding lower density and smaller size of loops.

3.3. Irradiation hardening

Table 2 also shows the irradiation hardening effects which are displayed for each sample, especially for W–26Re despite of the voids and dislocation loops that cannot be investigated. The hardening quantities induced by proton and neutron irradiation of 0.15 dpa are very close. The result shows that the combination of W with Re or Os reduces the level of irradiation hardening, but the hardness change does not feature a dependence on the increasing Re content.

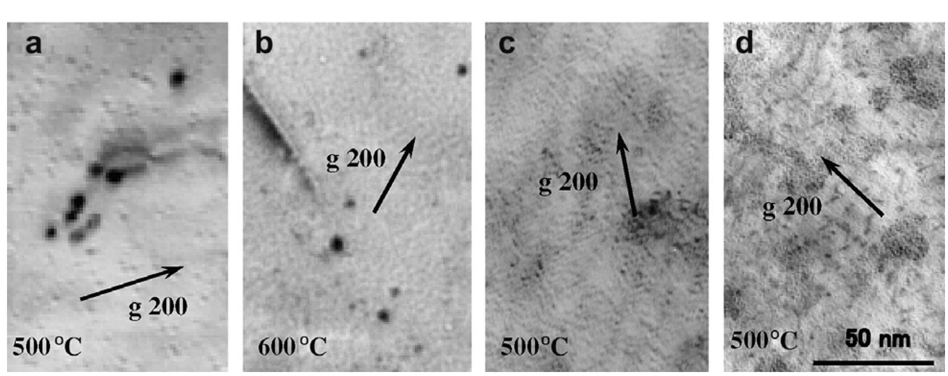

Fig. 2. Photographs showing loops to 0.15 dpa (E_n = 1 MeV) in proton-irradiated: (a) W, (b) W–3Re, (c) W–3Os and (d) W–5Re–3Os. No loops were observed in proton-irradiated W–3Os and W–5Re–3Os at 500 °C. The diffraction vector ($g = [200]$) is reached by tilting.

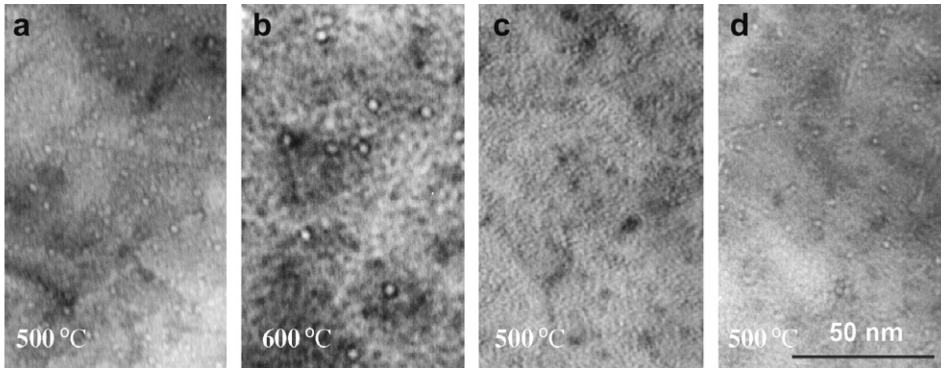

Fig. 3. Photographs showing voids to 0.15 dpa (E_n = 1 MeV) in proton-irradiated (a) W, (b) W–3Re, (c) W–3Os and (d) W–5Re–3Os. The higher irradiation temperature leads to void growth in (b). The voids in (c) are smaller than that in (d) even 5% Re is joined.

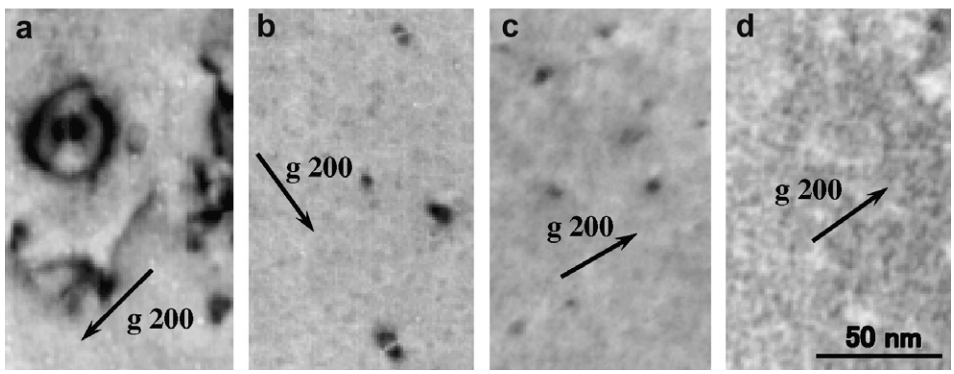

Fig. 4. Photographs showing loops at 600 °C to 0.15 dpa (E_n > 1 MeV) in neutron-irradiated: (a) W, (b) W–3Re, (c) W–5Re and (d) W–26Re. The diffraction vector (g = [200]) is reached by tilting.

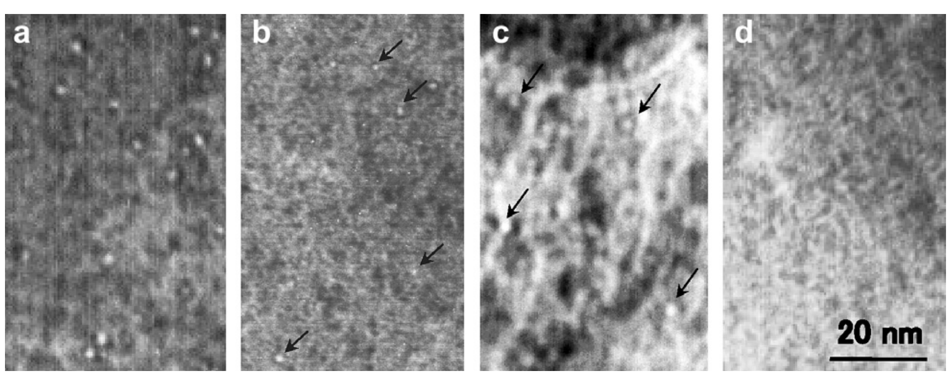

Fig. 5. Photographs showing voids at 600 °C to 0.15 dpa (E_n > 1 MeV) in neutron-irradiated: (a) W, (b) W–3Re, (c) W–5Re and (d) W–26Re. The arrows denote voids in (b) and (c).

4. Discussion

The embryo collection of vacancies and interstitials can begin to grow in three-dimensional manner under irradiation environment, causing nucleation of voids and dislocation loops. Generally, the alloying is seen to be improvable of nucleation energy for radiation-induced defects, and solute atom is able to obstacle the migration of defects. On the other hand, it is well known that the addition of Re to W can significantly improve the high temperature strength. As a comparison with the solute Re, our previous work showed the solute Os plays a more significant role in lattice dilation for W as larger solution induced hardening [9]. In the present work, the microstructural observation indicates that dislocation loops and voids are significantly decreased in number density because of the joint of Re or Os and their growth depends on the mobility of radiation-induced defects. Furthermore, Os gives a more significant influence in restrain of defect growth than Re. In both the Figs. 2 and 4, micrographs of proton-irradiated W–5Re–3Os and W–3Os and neutron-irradiated W–5Re and W–3Re indicate that the voids have little grown in size with corresponding decrease in number density because of the increasing Re content. We suggest that this is caused by which the radiation-induced vacancies tend to be collected around solute atoms, so that the increasing Re content can provide more opportunity for the void growth. However, the observation indicates that the solute atoms give more significant restrain effect on loop growth, and both number density and size are progressively decreased with the increasing solute content. Despite no loops and voids were observed in neutron-irradiated W–26Re, many small

Table 2
Proton and neutron-irradiated defects

	Voids		Loops		Vickers hardness difference
	Radius, nm	Density, $10^{22}/m^3$	Radius, nm	Density, $10^{21}/m^3$	$\Delta HV_{irrad} - \Delta HV_{unirrad}$
Proton-irradiated to 0.15 dpa					
W (500 °C)	1.8	13.9	3.8	1.9	185
W–3Re (600 °C)	2.2	5.6	3.4	1.3	105
W–3Os (500 °C)	1.1	13.5	–	–	89
W–5Re–3Os (500 °C)	1.4	9.8	–	–	–
Neutron-irradiated to 0.15 dpa					
W (600 °C)	1.3	6.4	7.9	4.6	207
W–3Re (600 °C)	1.1	3.4	3.6	1.4	71
W–5Re (600 °C)	1.2	2.1	3.2	1.5	80
W–26Re (600 °C)	–	–	–	–	87

defects are sure to be generated because irradiation hardening of irradiated W–26Re is also induced as other irradiated alloys.

As well known, ion particles ultimately remain in the implantation target to nucleate voids. In the present work the proton implantation depth was less than 7 μm (see Fig. 1). To compare these results with neutron irradiation, a larger size and higher number density of voids are indicated with corresponding smaller size loops by proton irradiation. A post-irradiation observation experiment using laser microscopy showed that the voids induced by the present proton irradiation in pure W first grew into gas bubbles while the temperature was rising, and then the bubbles were released outside from the W surface while the temperature rose to near 800 °C [11].

5. Summary

This work investigated the microstructure of proton and neutron irradiation under the same irradiation damage conditions of 0.15 dpa and evaluated the effects of transmutation elements Re and Os of W on the radiation-induced defect structure development. The following points summarize the results of this study.

(1) The combination of W with Re or Os could restrain the growth of radiation-induced defects, and Os played a more significant restrain effect than Re.
(2) The microstructure observation showed that more voids were induced by proton irradiation than by neutron irradiation because the protons tended to remain on the surface, but a higher number density and a larger size of dislocation loops were given in neutron-irradiated samples.
(3) Irradiation hardening was induced for each sample even in W–26Re where no voids and dislocation loops were observed. The largest irradiation hardening was given in irradiated W, and the level of irradiation hardening depended on the number density and size of radiation-induced defects.

Acknowledgement

Support for the fabrication and chemical composition analysis by the Institute for Material Research (IMR) of Tohoku University is deeply appreciated.

References

[1] V. Barabash, G. Federici, M. Rödig, L.L. Snead, C.H. Wu, J. Nucl. Mater. 283–287 (2000) 138.
[2] D.L. Smith, R.F. Mattas, M.C. Billone, in: R.W. Cahn et al. (Eds.), Materials Science and Technology, vol. 10B, VCH, New York, pp. 243–252.
[3] C.H. Wu, C. Alessandrini, R. Moormann, M. Rubel, B.M.U. Scherzer, J. Nucl. Mater. 220–222 (1995) 860.
[4] L.R. Greenwood, F.A. Garner, J. Nucl. Mater. 212–215 (1994) 635.
[5] C.B.A. Forty, G.J. Butterworth, J.-Ch. Sublet, J. Nucl. Mater. 212–215 (1994) 640.
[6] G.A. Cottrell, J. Nucl. Mater. 334 (2004) 166.
[7] J.C. He, A. Hasegawa, K. Abe, Mater. Trans. (submitted for publication).
[8] Y. Nemoto, A. Hasegawa, M. Satou, K. Abe, J. Nucl. Mater. 283–287 (2000) 1144.
[9] J.-C. He, A. Hasegawa, M. Fujiwara, M. Satou, T. Shishido, K. Abe, Mater. Trans. 45 (2004) 2600.
[10] J.P. Biersack, J.F. Ziegler, TRIM85 Program, IBM Corp. Yorktown, NY, 1985.
[11] M. Miyahara, Master Dissertation, Tohoku University, 2005.